1521-0111/100/1/7–18$35.00
MOLECULAR PHARMACOLOGY

https://doi.org/10.1124/molpharm.120.000076
Mol Pharmacol 100:7–18, July 2021

Differential In Vitro Pharmacological Profiles of Structurally Diverse Nociceptin Receptor Agonists in Activating G Protein and Beta-Arrestin Signaling at the Human Nociceptin Opioid Receptor[S]

James J. Lu, Willma E. Polgar, Anika Mann, Pooja Dasgupta, Stefan Schulz, and Nurulain T. Zaveri

Astraea Therapeutics, Mountain View, California (J.J.L., W.E.P., N.T.Z.); and Institute of Pharmacology and Toxicology, Jena University Hospital, Friedrich Schiller University Jena, Jena, Germany (A.M., P.D., S.S.)

Received May 29, 2020; accepted March 26, 2021

ABSTRACT

Agonists at the nociceptin opioid peptide receptor (NOP) are under investigation as therapeutics for nonaddicting analgesia, opioid use disorder, Parkinson's disease, and other indications. NOP full and partial agonists have both been of interest, particularly since NOP partial agonists show a reduced propensity for behavioral disruption than NOP full agonists. Here, we investigated the in vitro pharmacological properties of chemically diverse NOP receptor agonists in assays measuring functional activation of the NOP receptor such as guanosine 5'-O-[gamma-thio]triphosphate (GTPγS) binding, cAMP inhibition, G protein–coupled inwardly rectifying potassium (GIRK) channel activation, phosphorylation, β-arrestin recruitment and receptor internalization. When normalized to the efficacy of the natural agonist nociceptin/orphanin FQ (N/OFQ), we found that different functional assays that measure intrinsic activity produce inconsistent levels of agonist efficacy, particularly for ligands that were partial agonists. Agonist efficacy obtained in the GTPγS assay tended to be lower than that in the cAMP and GIRK assays. These structurally diverse NOP agonists also showed differential receptor phosphorylation profiles at the phosphosites we examined and induced varying levels of receptor internalization. Interestingly, although the rank order for β-arrestin recruitment by these NOP agonists was consistent with their ability to induce receptor internalization, their phosphorylation signatures at the time point we investigated were not indicative of the levels of β-arrestin recruitment or internalization induced by these agonists. It is possible that other phosphorylation sites, yet to be identified, drive the recruitment of NOP receptor ensembles and subsequent receptor trafficking by some nonpeptide NOP agonists. These findings potentially help understand NOP agonist pharmacology in the context of ligand-activated receptor trafficking.

SIGNIFICANCE STATEMENT

Chemically diverse agonist ligands at the nociceptin opioid receptor G protein–coupled receptor showed differential efficacy for activating downstream events after receptor binding, in a suite of functional assays measuring guanosine 5'-O-[gamma-thio]triphosphate binding, cAMP inhibition, G protein–coupled inwardly rectifying protein channel activation, β-arrestin recruitment, receptor internalization and receptor phosphorylation. These analyses provide a context for understanding nociceptin opioid peptide receptor (NOP) agonist pharmacology driven by ligand-induced differential NOP receptor signaling.

Introduction

The nociceptin/orphanin FQ receptor opioid (NOP) receptor is the last discovered member of the opioid G protein–coupled receptor (GPCR) family (Bunzow et al., 1994; Fukuda et al., 1994; Lachowicz et al., 1995; Mollereau et al., 1994) and is a G_i/G_o coupled receptor like the classic opioid receptors mu (MOR), delta, and kappa. The endogenous ligand for the NOP receptor is a heptadecapeptide, nociceptin/orphaninFQ (N/OFQ), which only binds the NOP receptor and has no affinity for the classic opioid receptors (Meunier et al., 1995; Reinscheid et al., 1995). As with classic opioid receptors, activation of NOP by N/OFQ or synthetic agonists leads to inhibition of adenylate cyclase and cAMP production, inhibition of calcium channels, and activation of G protein–coupled inwardly rectifying potassium (GIRK) channels (Hawes et al., 2000; Ikeda et al., 1997; Mollereau et al., 1994). Although they are not completely understood, key signal transduction pathways activated after ligand binding to the NOP GPCR have been investigated (Toll et al., 2016). Ligand binding to the cell surface NOP receptor leads to binding of the inhibitory heterotrimeric $G_{i/o}$ G protein, followed by dissociation of the Gα subunit, resulting in the inhibition of adenylate cyclase activity and

This work was supported by the National Institutes of Health National Institute on Drug Abuse [Grants R01DA027811 and R44DA042465 to N.T.Z.].
https://doi.org/10.1124/molpharm.120.000076.

[S] This article has supplemental material available at molpharm.aspetjournals.org.

ABBREVIATIONS: DMEM, Dulbecco's modified Eagle's medium; Emax, agonist efficacy; GIRK, G protein–coupled inwardly rectifying potassium channel; GPCR, G protein–coupled receptor; GRK, G protein receptor kinase; GTPγS, guanosine 5'-O-[gamma-thio]triphosphate; HA, human influenza hemagglutinin; HEK293, human embryonic kidney 293; hMOR, human mu opioid peptide receptor; hORL, human opioid receptor–like receptor; MOR, mu opioid peptide receptor; N/OFQ, nociceptin/orphanin FQ; NOP, nociceptin opioid peptide receptor.

decrease in the intracellular levels of cAMP. The G$\beta\gamma$ subunits couple to and activate GIRK channels, increasing potassium current (Connor et al., 1996a; Vaughan and Christie, 1996) and suppressing voltage-dependent calcium channels (Beedle et al., 2004; Connor et al., 1996b), resulting in cell hyperpolarization. This channel modulation upon agonist binding to the NOP receptor is consistent with the inhibitory actions of N/OFQ and agonists on neuronal activity and neurotransmitter release.

Like other GPCRs, NOP signaling and function are regulated by phosphorylation, internalization, and receptor desensitization (see Donica et al., 2013 for an excellent review). The G$\beta\gamma$ subunits that dissociate from the G protein–receptor complex recruit G protein receptor kinases (GRKs) for phosphorylation of GPCR intracellular domains. The agonist-bound phosphorylated GPCR undergoes a conformational change, allowing arrestin recruitment, receptor internalization, and desensitization, as shown for the MOR receptor (Williams et al., 2013). The NOP receptor contains several serine, threonine and tyrosine residues within its intracellular loops and C-terminal domain that can act as substrates for GRK-mediated NOP receptor phosphorylation. Using phosphosite specific antibodies, Mann et al. (2019) recently showed that NOP C-terminal residues Ser346, Ser351, and Thr362/Ser363 were phosphorylated after treatment with diverse NOP agonists in a spatial and temporal manner, with S346 being the first site of phosphorylation. GRK2 and GRK3 were shown to be important for agonist-induced phosphorylation and receptor desensitization (Mandyam et al., 2002; Mandyam et al., 2003; Mann et al., 2019; Thakker and Standifer, 2002). Furthermore, alanine mutation of S363, which is phosphorylated by GRK3, reduced β-arrestin2 recruitment and NOP internalization (Zhang et al., 2012).

Arrestin recruitment by nonpeptide NOP ligands has been investigated in a limited number of studies, some of which included NOP full agonist AT-403 and NOP partial agonists AT-090 and AT-004 characterized here (Chang et al., 2015; Ferrari et al., 2016; Ferrari et al., 2017; Malfacini et al., 2015). NOP full agonist AT-403 showed significant arrestin recruitment but also activated G protein–mediated recruitment to the same extent, similar to the endogenous agonist N/OFQ (Ferrari et al., 2017). On the other hand, NOP partial agonist AT-090 [21% agonist efficacy in the GTPγS binding assay; Ferrari et al., 2016] showed significant efficacy for arrestin recruitment (Ferrari et al., 2016), unlike NOP partial agonist AT-004, which also showed ∼20% agonist efficacy in GTPγS binding but was nearly inactive in recruiting β-arrestin (Chang et al., 2015; Ferrari et al., 2016; Malfacini et al., 2015). These NOP ligands have not been previously characterized for their effects on NOP receptor phosphorylation or internalization, but their differential efficacy of arrestin recruitment suggests that chemically diverse NOP agonists can have differential effects on NOP receptor signaling and trafficking. Here, we profiled phosphorylation signatures, arrestin recruitment, and receptor internalization induced by diverse NOP agonists. We also characterized the intrinsic activity of these ligands in mediating G protein–mediated downstream events. Commonly used assays to measure functional efficacy of opioid ligands in G protein–mediated signaling include simple proximal measurements of G protein recruitment like the GTPγS binding assay (McDonald and Lambert, 2010; Sim et al., 1996) as well as other assays of downstream signaling such as cAMP inhibition (Hill et al., 2010; Knapman et al., 2014), calcium release (Camarda et al., 2009; Coward et al., 1999), and GIRK activation (Parsons and Hirasawa, 2011). These assays often provide inconsistent measures of intrinsic activity for the same ligand, and such inconsistencies become particularly significant when agonist efficacy obtained in nonamplified assay systems such as GTPγS assays are compared with that obtained in amplified assay systems such as the cAMP and GIRK assays. Levels of agonist efficacy seen in different G protein assays can also be confounded by receptor reserve, as agonists can produce a maximum response by occupying only a fraction of receptors (Selley et al., 1998; Traynor and Nahorski, 1995; Gillis et al., 2020; Kelly, 2013). Receptor reserve can also account for signal amplification and confound experimental measures of agonist efficacy, particularly when characterizing partial agonists in heterologous transfected cells (Adham et al., 1993; Baker et al., 2000; Selley et al., 1998; Traynor and Nahorski, 1995).

Here, we investigated the functional efficacy of several selective NOP agonists from our NOP ligand library, using multiple G protein assays and determined the range of intrinsic activity obtained among various assays for the same ligand. We also investigated the phosphorylation profiles, arrestin recruitment, and receptor internalization induced by these selective NOP agonists and found differential ligand-induced NOP receptor signaling and trafficking among the NOP ligands we examined.

Materials and Methods

Chemical Compounds. NOP-selective ligands AT-004 (Kamakolanu et al., 2020), AT-090 (Ferrari et al., 2016), AT-200 (Zaveri et al., 2004), AT-312 (Zaveri et al., 2018b), AT-390 (Arcuri et al., 2018), and AT-403 (Arcuri et al., 2018) were synthesized at Astraea Therapeutics and have been previously reported. Stock solutions of N/OFQ at a 1 mM concentration and [D-Ala2, N-MePhe4, Gly-ol]-enkephalin (DAMGO) at a 10 mM concentration were prepared in deionized water, whereas those of the AT ligands were prepared in DMSO (10 mM) and diluted with water or assay medium to the desired concentration.

Cell Culture and Transfection. All cells were maintained in a 5% CO_2 incubator under saturated humidity and 37°C. Human NOP, or human opioid receptor–like receptor (hORL), and human MOR (hMOR) opioid receptors were stably expressed individually in CHO cells as reported previously (Zaveri et al., 2001). The hORL CHO cells were cultured in 150 mm tissue culture dishes (Corning, New York City, NY) in Dulbecco's modified Eagle's medium (DMEM; Gibco, Thermo Fisher Scientific, Waltham, MA) supplemented with 10% FBS, 100 U/ml penicillin, 100 μg/ml streptomycin and 400 μg/ml G418. The hMOR CHO cells were cultured in 50% F12/DMEM (Gibco, Thermo Fisher Scientific, Waltham, MA) supplemented with 10% FBS, 100 U/ml penicillin, 100 μg/ml streptomycin, and 400 μg/ml G418. The AtT-20/D16v-F2 (AtT-20) cells used in GIRK assays were purchased from the American Type Culture Collection and cultured in DMEM supplemented with 10% FBS, 2 mM L-glutamine, 100 U/ml penicillin, and 100 μg/ml streptomycin. The HTLA cells [a human embryonic kidney 293 (HEK293) cell line stably expressing a tetracycline-controlled transactivator-dependent luciferase reporter and a β-arrestin2–tobacco etch virus protease fusion gene used for β-arrestin assays were a gift from Dr. Bryan Roth and cultured in DMEM supplemented with 10% FBS, 100 U/ml penicillin, 100 μg/ml streptomycin, 100 μg/ml hygromycin B, and 2 μg/ml puromycin. Then, the HTLA cells were transiently transfected with NOP or MOR receptors overnight before the β-arrestin assays were carried

out (see details below). For cAMP assays, the hORL and hMOR CHO cells were transiently transfected with a cAMP23F plasmid (Promega, Madison, WI) overnight before the cAMP assays were carried out (see details below).

Membrane Preparation. The hORL and hMOR CHO cells were grown to confluency and harvested for membrane preparation. The membrane was prepared in 50 mM Tris buffer (pH 7.4). Cells were scraped off 150-mm culture dishes and centrifuged at 500*g* for 15 minutes. The cell pellet was homogenized in 50 mM Tris with a Fisher Scientific PowerGen 125 rotor-stator type homogenizer, centrifuged at 20,000*g* for 25 minutes, washed and recentrifuged once more at 20,000*g* for 25 minutes, aliquoted at a concentration of 2 mg/ml protein per vial for hORL and 3 mg/ml protein per vial for hMOR, and stored in a –80°C freezer until use.

Receptor Binding Assay. AT compounds were dissolved in 100% DMSO to a concentration of 10 mM. The binding assays were performed in 96-well polystyrene plates using six concentrations of each test compound (final concentration of 10 μM to 0.1 nM in 10-fold dilutions) in triplicate, with each well containing 100 μl of compound and 100 μl of tritiated ligands [^{3}H]DAMGO (48.0 Ci/mmol, K_d 0.69 nM for MOR) or [^{3}H]N/OFQ (130 Ci/mmol, K_d 0.065 nM for NOP). Nonspecific binding was determined using 1.0 μM of the unlabeled nociceptin for NOP and 1.0 μM of unlabeled DAMGO for MOR. Assays were initiated by the addition of 800 μl of membrane per well, after which the samples were incubated for 60 minutes at 25°C in a total volume of 1.0 ml. In NOP receptor experiments, 1 mg/ml bovine serum albumin was added to the compound dilution buffer. The incubation was terminated by rapid filtration through 0.05% polyethylenimine-soaked glass fiber filter mats (GF/C Filtermat A, Perkin Elmer) on a Tomtec Mach III cell harvester and washed 5 times with 0.5 ml of ice-cold 50 nM Tris-HCl (pH 7.4) buffer. The filters were dried overnight and soaked with scintillation cocktail before counting on a Wallac Beta plate 1205 liquid scintillation counter. Radioactivity was determined as counts per minute. IC_{50} values were determined using at least six concentrations of test compound and calculated using the variable slope curve-fitting method in GraphPad Prism 6.0 software (ISI, San Diego, CA). K_i values were determined by the method of Cheng and Prusoff (Cheng and Prusoff, 1973).

[^{35}S] GTPγS Binding Assay. [^{35}S] GTPγS binding assays were conducted as previously described (Khroyan et al., 2011; Toll et al., 2009). In brief, membranes (2 mg/ml protein for NOP and 3 mg/ml for MOR) were incubated for 60 minutes at 25°C with [^{35}S] GTPγS (50 pM), GDP (10 μM), and the appropriate compound, in a total volume of 1.0 ml Buffer A containing 20 mM HEPES, 10 mM $MgCl_2$, and 100 mM NaCl (pH 7.4). Samples were filtered over glass fiber filters and counted as described for the binding assays. Agonist efficacy (Emax) is reported as percentage of maximal stimulation relative to the standard full agonist N/OFQ or DAMGO and calculated as maximal stimulation by test compound ÷ maximal stimulation by standard full agonist ×100. The EC_{50} values were calculated using the variable slope dose-response curve fitting method in GraphPad Prism 6.0 software.

GloSensor cAMP Assay. The plasmid pGloSensor-23F-cAMP was transfected into hORL and hMOR CHO cells (1.5×10^6 cells) using the Fugene 6 HD reagent (Promega, Madison, WI). Twenty-four hours after the transfection, the cells were harvested, suspended in the culture medium, and seeded (100 μl/well at a concentration of 1×10^5 cells/ml) into 96-well white wall microtiter plates. After being incubated at 37°C for 24 hours in a humidified environment containing 5% CO_2, the medium was replaced with DMEM containing 6% GloSensor cAMP substrate (Promega, Madison, WI). After 2 hours of additional incubation at room temperature, different AT compounds at five concentrations (final concentration of 1 μM to 0.1 nM in 10-fold dilutions) were added into the wells for 15 minutes of incubation, followed by the addition of 10 μM of forskolin (final concentration) to stimulate cAMP synthesis. Then, the dynamic luminescence signal of the wells was detected immediately using a FluoStar Optima plate reader (BMG, Gütersloh, Germany) for 30 consecutive minutes at a rate of 1 read per well per second. Subsequently, to calculate Emax of the standard agonist, cAMP inhibition induced by 1 μM of the positive control N/OFQ or DAMGO in the presence of 10 μM of forskolin (i.e., the max level of cAMP signal in the presence of 1 μM N/OFQ or DAMGO plus 10 μM forskolin divided by the max level of cAMP signal in the presence of 10 μM forskolin only) was used as 100%, and the level of cAMP inhibition induced by test compounds was normalized to that of N/OFQ or DAMGO (net cAMP inhibition by test compound ÷ net cAMP inhibition by 1 μM full agonist × 100). In addition, the IC_{50} of different compounds in inhibiting cAMP synthesis was calculated using the variable slope dose-response curve fitting method in GraphPad Prism 6.0 software. To minimize intra-assay variations caused by transient transfections carried out on different days, the key time points of the assay, including the time of transfection, the time of compound, forskolin, and reagent addition, and the time of signal readout on the plate reader, were kept the same among different days. Furthermore, only the experiments showing comparable baseline (negative control) and positive control (N/OFQ or DAMGO) signals were included in the comparative analyses to ensure intra-assay consistency.

GIRK Assay. AtT-20 cells stably expressing hNOP or hMOR receptors were plated in 96-well black, clear bottom plates covered with poly-L-lysine. Plates were kept for 48 hours at 37°C and 5% CO_2. Assay was performed as previously described (Günther et al., 2016) using Hanks' balanced salt solution, buffered with HEPES 20 mM (pH 7.4) as standard buffer. The membrane potential dye FMP (FLIPR Membrane Potential kit BLUE, Molecular Devices, Biberach, Germany) was reconstituted according to manufacturer's instructions. Test compounds were prepared right before assay measurements at the concentration indicated. The assay was performed in a FlexStation 3 microplate reader (Molecular Devices, Biberach, Germany).

Western Blot Analysis (Receptor Phosphorylation). Stably transfected HEK293 cells expressing human NOP receptors were plated onto poly-L-lysine–coated 60-mm dishes and grown for 2 days to 80% confluency. After incubating with 10 μM N/OFQ or agonists for 10 minutes at 37°C, the cells were lysed with a detergent buffer (50 mM Tris-HCl, pH 7.4; 150 mM NaCl; 5 mM EDTA; 10 mM NaF; 10 mM disodium pyrophosphate; 1% Nonidet P-40; 0.5% sodium deoxycholate; 0.1% SDS) in the presence of protease and phosphatase inhibitors. After 30 minutes of centrifugation at 4°C, human influenza hemagglutinin (HA)-tagged NOP receptors were enriched using anti-HA–agarose beads. Samples were then inverted for 1.5 hours at 4°C. After washing, proteins were eluted using an SDS sample buffer for 30 minutes at 50°C, and proteins were separated on 7.5% or 12% SDS-polyacrylamide gels. After electroblotting, membranes were incubated with either 0.1 g/ml anti–human phosphorylated S346 (5034), anti–human phosphorylated S351 (4876), or anti–human phosphorylated T362/S363 (4874) antibodies overnight at 4°C, followed by detection of bound antibodies using an enhanced chemiluminescence buffer (Thermo Fisher Scientific, Schwerte, Germany). Blots were subsequently stripped and reprobed with the phosphorylation-independent anti–NOP receptor antibody (4871) or anti-HA antibody (0631) to ensure equal loading of the gels.

Analysis of NOP Receptor Internalization. Stably transfected cells expressing HA-tagged human NOP receptors were plated onto poly-L-lysine–coated coverslips and grown overnight. Cells were incubated with rabbit anti-HA antibody (0631) in serum-free medium for 2 hours at 4°C. After 60 minutes of agonist exposure at room temperature, cells were fixed with 4% paraformaldehyde and 0.2% picric acid in a phosphate buffer (pH 6.9) for 30 minutes at room temperature. Subsequently, cells were washed several times with a phosphate buffer (22.6 ml/L 1M $NaH_2PO_4 \bullet H_2O$; 77.4 ml/L 1M $Na_2HPO_4 \bullet H_2O$; 0.1% Triton X-100, pH 7.4), permeabilized, and then incubated with an Alexa488-coupled goat anti-rabbit antibody (Invitrogen, Darmstadt, Germany). Cells were mounted, and the internalization of receptors was examined using a Zeiss LSM510 META laser scanning confocal microscope (Jena, Germany).

For quantitative internalization assays, cells were plated onto 24-well plates and grown overnight. Then, the cells were preincubated with anti-HA antibody (0631) for 2 hours at 4°C and exposed to agonists for 60 minutes at 37°C. Subsequently, cells were fixed for 45 minutes at room temperature, washed three times with PBS, and incubated with a peroxidase-conjugated secondary antibody (Santa Cruz, Heidelberg, Germany). After washing, ABTS substrate [2,2′-azino-bis(3-ethylbenzothiazoline-6-sulfonic acid) diammonium salt] was added, and optical density was measured at 405 nm using a FlexStation 3 microplate reader (Molecular Devices, Biberach, Germany).

β-Arrestin Recruitment Assay. The β-arrestin recruitment assay was carried out based on the method described previously (Allen et al., 2011). In brief, on the night prior to transfection (day 1), HTLA cells were plated at 10×10^6 cells in 150-mm cell culture dishes (Corning, New York City, NY). On the following day when cells grew to 80% confluency (day 2), the cells were transfected with human NOP or MOP receptors using the Fugene 6 HD transfection reagent (Promega, Madison, WI) following the protocol provided by the manufacturer. The ratio of DNA plasmid to Fugene 6 HD transfection reagent in the transfection was 1 μg DNA:6 μl Fugene 6 HD. Thirty micrograms of DNA was used for the transfection of cells in each culture dish. After 24 hours of transfection (day 3), transfected cells were harvested by trypsinization (Trypsin-EDTA, Gibco, Thermo Fisher Scientific, Waltham, MA) and then seeded into white flat-bottom 96-well tissue culture plates (Corning, New York City, NY) at 5×10^4 cells per well. Twenty-four hours later (day 4), the cells were treated with AT compounds or positive controls (DAMGO or N/OFQ for MOR and NOP, respectively) for 18 hours at 37°C. On day 5, the luciferase signal in each well was detected by using a Bright Glo Luciferase Reporter Assay (Promega, Madison, WI) on a plate reader (BMG, FluoStar Optima, Gütersloh, Germany). The level of β-arrestin recruitment was determined by subtracting the baseline signal (medium only) from the signal detected in the presence of compound. Furthermore, to calculate percentage of β-arrestin recruitment, the amount of β-arrestin recruitment induced by the positive control N/OFQ/DAMGO (1 μM) was used as 100%, and the amount of β-arrestin recruitment induced by AT compounds was normalized to that of N/OFQ or DAMGO. In addition, the EC_{50} values were calculated using the variable slope dose-response curve fitting method in GraphPad Prism 6.0 software. Each experiment was repeated at least three times, with each drug concentration in quintuplicate wells to obtain and report the average value ± S.D. Similar to our approach in the cAMP inhibition assay, we carried out the operations of the β-arrestin recruitment assay at fixed time points to minimize intra-assay variations. We also only included the experiments showing comparable baseline (negative control) and positive control (N/OFQ or DAMGO) signals for comparison.

Data Analysis. Experimental data in Tables 1–3 are expressed as means ± S.D. IC_{50} and EC_{50} values were calculated with GraphPad Prism 6.0 (GraphPad software, La Jolla, CA) using the respective curve-fitting methods indicated in the *Materials and Methods*. S.D. was derived using the S.D. function (stdev) in Excel software. For Western blot assays, the detected protein bands were quantified using ImageJ version 1.47 software (National Institutes of Health, Bethesda, MD). Statistical analysis for Fig. 3C was carried out with Student's *t* test. A *P* value of <0.05 was considered statistically significant. Since this was an exploratory study, a graphical representation was used to compare ligand efficacies between β-arrestin recruitment and internalization, as shown in Fig. 5.

Results

Binding Affinity of AT Compounds for NOP and MOR Receptors. All tested NOP agonists (Fig. 1) showed high binding affinity with K_i values ranging from 0.3 to 9.8 nM at the recombinant NOP receptor and from 6.0 to 375.5 nM at the recombinant MOR receptor expressed in CHO cells (Table 1). Ligands were grouped into highly selective NOP ligands with NOP selectivity >35-fold over the MOR receptor (AT-403, AT-390, and AT-004) and modestly selective NOP ligands with NOP selectivity ranging from 17- to 26-fold (AT-200, AT-312, and AT-090) over the MOR receptor.

Intrinsic Activity in the GTPγS Binding Assay at NOP and MOR Receptors. Agonist potency and efficacy were measured in the GTPγS binding assay using membranes from CHO cells expressing human NOP or MOR receptors. Percentage of stimulation was determined by normalization to maximum activity elicited by standard full agonists N/OFQ and DAMGO. At NOP, AT-312, AT-390, and AT-403 displayed full agonist efficacy (~100% of the standard N/OFQ), whereas AT-200 > AT-004 > AT-090 showed less than 50% efficacy compared with N/OFQ (Table 2; Supplemental Figure 1). Based on this, the compounds were grouped into NOP full agonists (AT-312, AT-390, and AT-403) and NOP partial agonists (AT-004, AT-200, and AT-090) (Table 2). With respect to potency, the EC_{50} values of all compounds at NOP were consistently greater than their K_i values (Adapa and Toll, 1997). At MOR, all compounds showed significantly lower potency as well as lower efficacy compared with standard agonist DAMGO, consistent with their lower binding affinity at MOR.

cAMP Assay at NOP and MOR Receptors. In hORL or hMOR CHO cells transiently expressing the cAMP plasmid, both N/OFQ and DAMGO decreased forskolin-induced cAMP accumulation, yielding potencies (EC_{50}) of 2.2 nM for N/OFQ and 9.1 nM for DAMGO, respectively (Table 2; see also graphs of cAMP experiments in Supplemental Fig. 2). All AT compounds displayed high efficacy (85%–106%) relative to N/OFQ at the NOP receptor, in rank order AT-403 > AT-090 > AT-390 > AT-312 > AT-200 > AT-004 (Table 2). Notably, the potencies for all the compounds in the NOP cAMP assay were consistently higher compared with those obtained in the GTPγS binding assay (Table 2). Furthermore, although the NOP full agonists in the GTPγS assay (AT-312, AT-390, and AT-403) also showed full agonist efficacy in the cAMP assay, the AT compounds that showed partial agonist efficacy at NOP in the GTPγS assay (AT-004, AT-090, and AT-200) all showed nearly full agonist efficacy, but lower potencies than N/OFQ (Table 2), with exception of AT-090, which showed significantly increased potency and full agonist efficacy in the cAMP assay compared with the GTPγS binding assay.

At the MOR receptor, efficacy of the compounds obtained in the cAMP assay was also higher than that obtained via the GTPγS binding assay (Table 2), although the differences were less pronounced since these compounds had lower potency and efficacy at the MOR overall.

GIRK Channel Activation by AT Compounds at NOP and MOR Receptors. In the GIRK assay in AtT-20 cells expressing NOP or MOR receptor, both N/OFQ and DAMGO induced agonist-dependent membrane hyperpolarization in a concentration-dependent manner, yielding EC_{50} values of 1.2 nM for N/OFQ and 1.0 nM for DAMGO (Table 2), respectively, consistent with potencies we previously reported for these agonists (Mann et al., 2019). The AT compounds tested in this assay all displayed full agonist efficacy (95%–105%) at NOP receptor compared with N/OFQ, in rank order AT-312 > AT-200 > AT-004 (see also graphs in Supplemental Fig. 3). Moreover, similar to the observations in the cAMP assay, the EC_{50} (potency) values from the GIRK assay at the NOP

TABLE 1
Receptor binding affinities of NOP ligands at the human NOP and human MOR receptors expressed in CHO cells

Binding affinities were determined using radioligand displacement assays as described in *Materials and Methods*. Equilibrium dissociation constants (K^i) were derived from IC^{50} values using the Cheng-Prusoff equation. Each K^i value represents the arithmetic mean ± S.D. calculated from corresponding number of independent experiments, with each experiment performed in triplicate.

Compound	hNOP K_i nM (number of independent experiments)	hMOR K_i nM (number of independent experiments)	Selectivity (hMOR K_i/hNOP K_i) fold over hMOR binding
N/OFQ	0.12 ± 0.01[a]	—	—
DAMGO	—	0.59 ± 0.03[a]	—
AT-004	9.8 ± 0.9 (4)	375.5 ± 36.5 (4)	38-fold
AT-090	5.6 ± 1.7 (3)	95.4 ± 3.5 (3)	17-fold
AT-200	4.1 ± 0.1 (4)	107.1 ± 8.9 (7)	26-fold
AT-312	0.3 ± 0.1 (6)	6.0 ± 1.0 (6)	20-fold
AT-390	0.9 ± 0.3 (5)	53.1 ± 16.5 (5)	59-fold
AT-403	1.1 ± 0.1 (4)	97.9 ± 15.0 (7)	91-fold

[a]The number of N/OFQ and DAMGO binding experiments was not labeled since each experiment of AT compounds was accompanied with N/OFQ or DAMGO as the standard.

receptor were consistently shifted to lower values (higher potency) compared with those obtained in the GTPγS binding assay (i.e., the compounds appeared more potent in the GIRK assay than in the GTPγS functional assay). Furthermore, the efficacies of the compounds obtained from the GIRK assay were also higher than those obtained in the GTPγS binding assay. For example, AT-004 appears to be a low-efficacy partial agonist at NOP in the GTPγS assay but showed nearly full agonist efficacy and higher potency in the NOP GIRK assay.

The differences in the levels of intrinsic activity at NOP obtained from the GTPγS binding assay, GIRK assay, and cAMP assay for selected NOP ligands (AT-004, AT-200, and AT-312) are shown in Fig. 2. It can be seen that the intrinsic activity observed in the GIRK and cAMP assays are significantly higher than the stimulation achieved by these compounds in the GTPγS binding assay, especially for compounds behaving as partial agonists in the GTPγS assay, i.e., a stimulation level of 20%–60% (AT-004 and AT-200). AT-090 (Table 2) also showed partial agonist efficacy in the GTPγS assay (21% stimulation) but showed full agonist efficacy (104% stimulation) and significantly higher potency in the cAMP assay. NOP partial agonists AT-004 and AT-200 also showed significantly higher potencies in the GIRK assay compared with that in the GTPγS assay (Table 2).

On the other hand, the compounds displayed lower efficacy at the MOR receptor in the GIRK assay, in rank order AT-200 > AT-312 > AT-004, compared with DAMGO, and the efficacy and potency obtained from the GIRK assay appeared to be somewhat consistent with those observed in the GTPγS assay. This is particularly true for the low-efficacy partial agonist AT-004, which showed low efficacy and poor potency at MOR in the GTPγS assay and showed no GIRK channel activation (Table 2).

Phosphorylation of NOP Receptors Induced by AT Compounds. Using phosphosite-specific antibodies that we generated against residues in the NOP C-terminal tail, we previously showed that N/OFQ-induced NOP receptor phosphorylation occurs in a time-dependent manner, where S346 phosphorylation occurred within 20 seconds, S351 phosphorylation occurred within 60 seconds, and T362/S363 phosphorylation

TABLE 2
Functional assays of G protein signaling

	GTPγS		cAMP		GIRK	
Compound	EC_{50} nM	Emax %Stim	EC_{50} nM	Emax %Stim	EC_{50} nM	Emax %Stim
hNOP						
N/OFQ	3.6 ± 0.7	100	2.2 ± 1.8	100	1.2 ± 0.2	100
DAMGO	—	—	—	—	N.A.	< 5.0
hNOP full agonists						
AT-312	29.9 ± 1.4	102.3 ± 0.8	14.9 ± 7.6	98.0 ± 12.9	1.8 ± 0.2	105.8 ± 3.4
AT-390	15.2 ± 0.4	110.1 ± 11.4	12.6 ± 1.3	98.3 ± 5.8	ND	ND
AT-403	6.3 ± 1.4	104.6 ± 1.2	3.7 ± 4.5	105.9 ± 4.1	ND	ND
hNOP partial agonists						
AT-004	266.6 ± 73.7	39.7 ± 4.5	224.8 ± 123.4	84.8 ± 19.9	11.2 ± 2.7	97.9 ± 4.5
AT-090	50.1 ± 6.4	21.0 ± 6.5	4.5 ± 2.1	104.6 ± 11.6	ND	ND
AT-200	27.2 ± 0.8	55.5 ± 0.7	23.6 ± 11.3	89.3 ± 6.6	3.2 ± 0.6	99.0 ± 3.4
hMOR						
N/OFQ	—	—	—	—	N.A.	< 5.0
DAMGO	32.6 ± 4.1	100	9.1 ± 4.9	100	1.0 ± 0.2	100
AT-004	231.7 ± 10.3	16.3 ± 7.6	N.A.	13.3 ± 0.3	N.A.	< 5.0
AT-090	N.A.	6.0 ± 2.8	354.9 ± 75.9	84.7 ± 7.8	ND	ND
AT-200	68.0 ± 9.3	43.5 ± 14.7	59.2 ± 31.1	87.4 ± 2.7	75.4 ± 42.0	59.3 ± 4.8
AT-312	81.5 ± 16.0	24.6 ± 2.4	378.4 ± 28.4	60.4 ± 12.0	149.2 ± 32.6	76.2 ± 2.8
AT-390	143.8 ± 0.6	54.3 ± 9.4	100.3 ± 26.0	88.4 ± 1.0	ND	ND

%Stim indicates percentage of stimulation compared with that of the control N/OFQ or DAMGO, as described in *Materials and Methods*. N.A., not detectable; ND, not done. All results are expressed as means ± S.D. calculated from at least 3 independent experiments.

TABLE 3
Functional assays of phosphorylation, internalization, and β-arrestin recruitment

			hNOP		hMOR	
			β-arrestin recruitment		β-arrestin recruitment	
Compound	Phosphorylation intensity	Internalization %	EC_{50} nM	Recruitment %	EC_{50} nM	Recruitment %
N/OFQ	+	100	14.3 ± 9.0	100 ± 2.7	—	—
DAMGO	–	—	—	—	46.5 ± 22.7	100 ± 1.3
AT-004	–	50	N.A.	26.7 ± 8.4	N.A.	6.6 ± 0.1
AT-090	low	74	17.8 ± 12.3	146.3 ± 37.4	175.0 ± 80.3	84.4 ± 7.2
AT-200	low	25	241.0 ± 56.2	41.3 ± 4.7	29.6 ± 27.1	45.1 ± 2.9
AT-312	–	50	6.8 ± 3.5	97.3 ± 10.7	175.0 ± 28.2	84.5 ± 9.8
AT-390	–	122	6.3 ± 4.5	247.4 ± 64.8	165.0 ± 2.1	78.9 ± 4.1
AT-403	+	65	4.3 ± 3.2	77.8 ± 12.1	475.0 ± 196.0	92.1 ± 7.3

Recruitment: Percentage of β-arrestin recruitment compared with that induced by the control N/OFQ or DAMGO, as described in *Materials and Methods*. "–" indicates no phosphorylation, "+" indicates strong phosphorylation, "low" indicates a low level of phosphorylation between 10% and 30%. N.A., not available. The EC_{50} and Recruitment values of β-arrestin recruitment are expressed as means ± S.D. calculated from at least 3 independent experiments.

occurred after 3 minutes (Mann et al., 2019). Several known NOP agonists were also found to show varying profiles of phosphorylation after a 10-minute exposure (Mann et al., 2019). Using the same phosphosite-specific antibodies, we next investigated the phosphorylation signatures of the AT NOP full agonists and partial agonists at a single time point, i.e., after exposure for 10 minutes, and at different concentrations. Figure 3 shows that NOP full agonist AT-403 induced strong phosphorylation at S346, S351, and T362/S363 (Fig. 3A) at 10 μM concentration after a 10-minute exposure, similar to N/OFQ. NOP full agonist AT-312, however, showed phosphorylation only at S346 and S351 at 1 and 10 μM concentrations but no detectable phosphorylation at T362/S363 (Fig. 3A) when measured at this single time point (i.e., after 10 minutes of incubation). Interestingly, NOP full agonist AT-390 showed no detectable phosphorylation at any of the three phosphosites at any concentration after 10 minutes of incubation (Fig. 3A).

On the other hand, NOP partial agonists AT-004 and AT-200 showed no phosphorylation at 10 μM concentration at S351 and T362/S363 after 10 minutes of incubation (Fig. 3A), but partial agonist AT-090 showed dose-dependent phosphorylation at all three sites, albeit more robust phosphorylation at S346 compared with the other two sites S351 and T362/S363 (Fig. 3A).

Among the NOP full agonists examined here, only AT-403 was able to induce a multisite phosphorylation profile similar to that of the endogenous agonist N/OFQ at all three sites

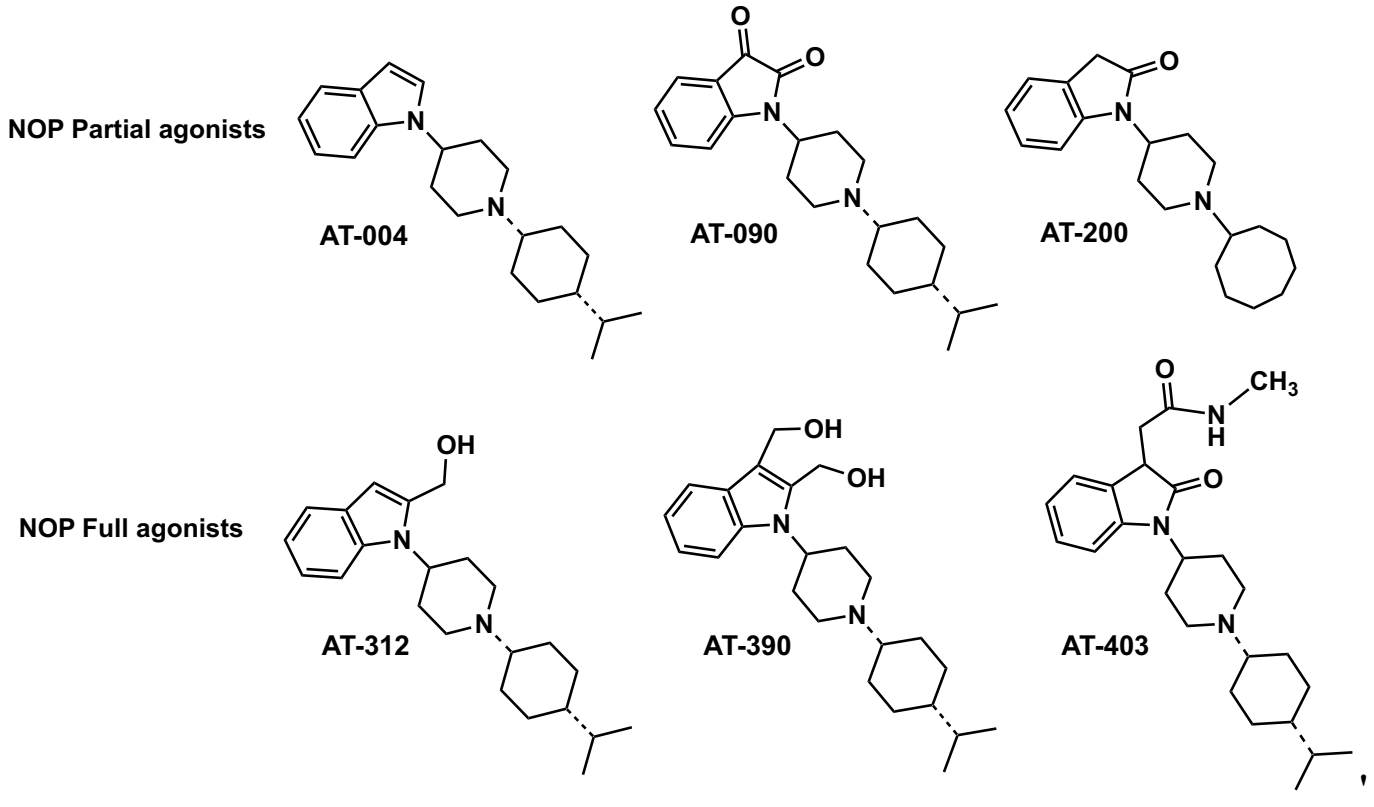

Fig. 1. Chemical structures of NOP agonists investigated.

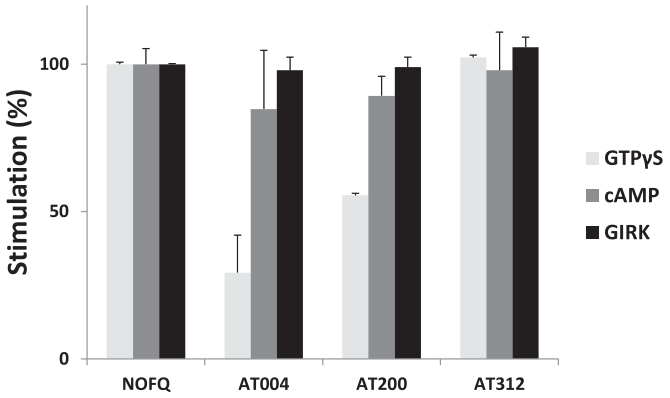

Fig. 2. Maximal stimulation of G protein signaling of human NOP receptor by NOP agonists, measured in GTPγS, cAMP and GIRK assays, and normalized to N/OFQ (100%). Each value represents the average value and S.D. obtained from three experiments done on different days, with triplicates in each experiment.

probed within 10 minutes of incubation. In this regard, AT-403 appears to have a similar phosphorylation signature to other known NOP agonists that we have previously investigated (Ro64-6198, SCH221510, AT-202, and MCOPPB; Mann et al., 2019) at similar time points. It is further notable that, under these same conditions, NOP full agonist AT-390 induces no phosphorylation at the three phosphosites we probed, whereas full agonist AT-312 shows no receptor phosphorylation at T362/S363 but induces phosphorylation at the other two sites. These results indicate that at the 10-minute time point, diverse NOP full agonists AT-403, AT-312, and AT-390 show differential but distinct receptor phosphorylation signatures.

Internalization of NOP Receptors Induced by AT Compounds. NOP receptor internalization was visualized by fluorescence microscopy and quantified using a cell surface ELISA (Fig. 3B and 3C). In time-course experiments, we previously showed that NOP receptor internalization was first detectable after 5 minutes of agonist treatment and reached a maximum after 60 minutes (Mann et al., 2019). In initial experiments, internalization by N/OFQ, NOP full agonists AT-312, and partial agonists AT-004 and AT-200 was qualitatively characterized using fluorescence confocal microscopy (Fig. 3B) after 60 minutes of agonist treatment. In subsequent experiments, internalization by N/OFQ, NOP full agonists AT-403 and AT-390, and partial agonist AT-090 after a 60-minute treatment was characterized by a quantitative ELISA (Fig. 3C). Figure 3B shows that N/OFQ induces robust internalization of the NOP receptor after 60 minutes of agonist exposure, further quantified by ELISA (in Fig. 3C) as the percentage of internalized receptors in N/OFQ-treated cells. NOP full agonist AT-403, which showed a similar multisite phosphorylation profile as N/OFQ after a 10-minute exposure, showed a significantly lower level of receptor internalization compared with N/OFQ (Fig. 3C) after the 60-minute exposure. In Fig. 3B, NOP full agonist AT-312, which also showed robust phosphorylation, appeared to show lower internalization compared with N/OFQ. On the other hand, NOP full agonist AT-390, which showed no phosphorylation (Fig. 3A) after the 10-minute exposure, showed a level of receptor internalization not significantly different from that of N/OFQ itself (Fig. 3C).

NOP partial agonist AT-090, which showed robust phosphorylation at S346 (Fig. 3A), showed receptor internalization not significantly different than N/OFQ (Fig. 3C), whereas partial agonists AT-004 and AT-200 showed little internalization of the NOP receptor (Fig. 3B) after the 60-minute exposure but also did not show phosphorylation at S351 or T362/S363.

Taken together, these results suggest that NOP phosphorylation at S346, S351, and T362/S363 may be sufficient, but not the only phosphorylated residues, to induce receptor internalization and that phosphorylation at other as yet unidentified residues in the intracellular domains of the NOP receptor is likely involved in receptor internalization induced by compounds such as AT-390. The lower internalization observed with full agonist AT-403 compared with N/OFQ and AT-390, and the higher phosphorylation and internalization seen with partial agonist AT-090 compared with AT-004 and AT-200, further suggest that structurally diverse NOP ligands may induce differential receptor trafficking and receptor desensitization.

β-Arrestin Recruitment of AT Compounds via NOP and MOR Receptors. β-arrestin recruitment by selective NOP agonists is shown in Table 3 and in graphs shown in Supplemental Fig. 4. The potency (EC_{50}) of the ligands and the percentage of stimulation of β-arrestin recruitment normalized to that by N/OFQ are shown in Fig. 4. NOP full agonist AT-403 showed significant β-arrestin recruitment with potency higher than that of N/OFQ, but with slightly lower efficacy (77% of N/OFQ recruitment). This lower efficacy for arrestin recruitment by AT-403 appears to be consistent with the lower percentage of internalization observed with AT-403 compared with that of N/OFQ. NOP full agonist AT-390, which shows comparable NOP internalization (but not phosphorylation), shows significant β-arrestin recruitment with potency higher than N/OFQ itself (Table 3). NOP full agonist AT-312 also shows nearly the same recruitment of β-arrestin with similar potency as N/OFQ. The rank order of β-arrestin recruitment by the synthetic NOP full agonists (AT-390 > AT-312 > AT-403) appears to be consistent with that for receptor internalization (AT-390 > AT-403), but not phosphorylation, particularly for AT-312 and AT-390. Among NOP partial agonists, AT-090 shows higher stimulation of arrestin recruitment than N/OFQ itself (Table 3; Supplemental Fig. 4). More importantly, even though AT-090 is a partial agonist of lower potency in the GTPγS assays, it shows the same potency as N/OFQ in the β-arrestin recruitment assay. Partial agonists AT-004 and AT-200 induced weak β-arrestin recruitment less than 50% of that induced by N/OFQ, and this appeared consistent with both their phosphorylation and internalization profiles.

At the MOR receptor, the selective NOP agonists AT-403, AT-390, and AT-312 had much lower potency for β-arrestin recruitment compared with the standard MOR agonist DAMGO (Table 3). Selective NOP partial agonist AT-004 showed undetectable recruitment of β-arrestin (Table 3). Modestly selective NOP partial agonist AT-200, which showed significant MOR partial agonist efficacy in the GTPγS assay and nearly full agonist efficacy in the GIRK assay (Table 2), had comparable potency for β-arrestin recruitment to MOR agonist DAMGO, albeit with lower efficacy (45% of DAMGO recruitment).

Overall, the efficacies of β-arrestin recruitment by the NOP agonists appeared to be associated with the levels of

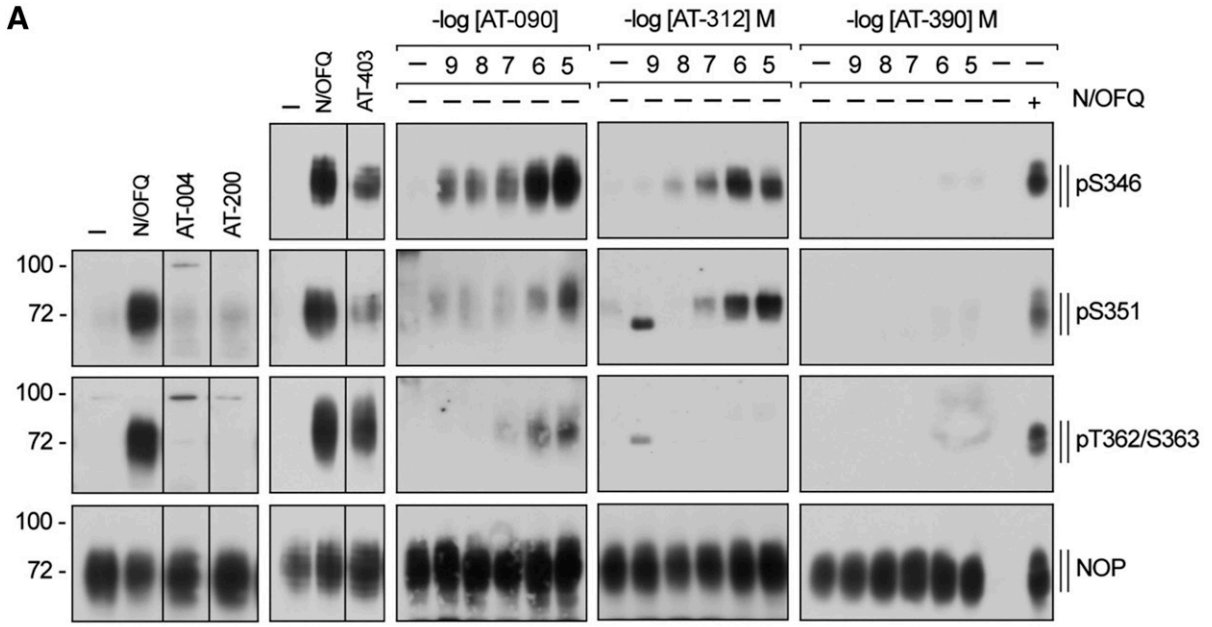

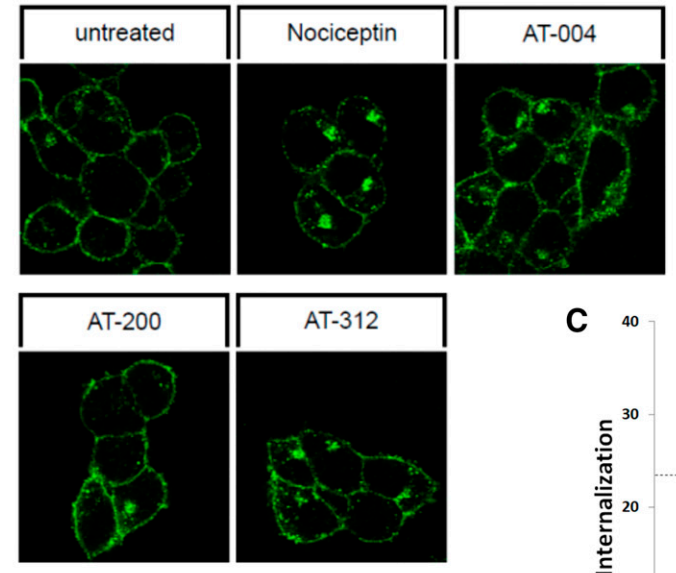

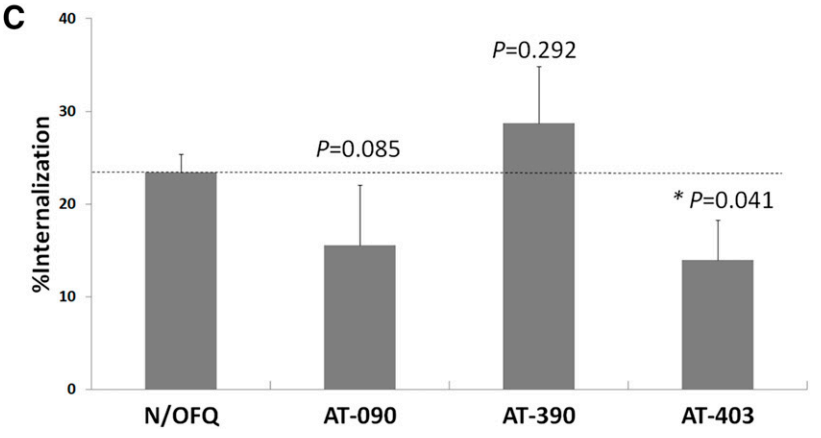

Fig. 3. Phosphorylation and internalization induced by AT compounds at human NOP receptor. (A) HEK293 cells expressing human NOP receptors were treated with 10 μM of N/OFQ, AT-004, AT-200, AT-403, or vehicle (–) or with 1 nM to 10 μM of AT-090, AT-312, and AT-390, at 37°C for 10 minutes, and cell lysates were immunoblotted with antibodies to phosphorylated (p) S346, pS351, or pT362/S363. Blots were stripped and reprobed for human NOP receptor to ensure equal loading. All blots were representative of 3–5 experiments. (B) HEK293 cells stably expressing HA-tagged human NOP receptors were preincubated with HA antibody and then stimulated with 10 μM of N/OFQ, AT-004, AT-200, AT-312, or solvent vehicle at 22°C for 60 minutes. Cells were then fixed, permeabilized, stained immunofluorescently, and examined subsequently using confocal microscopy. All images were representative of three independent experiments. (C) HEK293 cells stably expressing human NOP receptors were preincubated with antibody to HA-tag and treated with 10 μM of N/OFQ, AT-390, AT-090, or AT-403 at 37°C for 60 minutes. Then, the cells were fixed and labeled with a peroxidase-conjugated secondary antibody. Receptor internalization was measured by ELISA and quantified as the percentage of internalized receptors in the cells treated with agonists. Data represent means ± S.D. from 12 independent experiments performed in quadruplicate. The P values were comparative with N/OFQ and were obtained using two sample Student's t tests assuming unequal variances. *$P < 0.05$ versus N/OFQ.

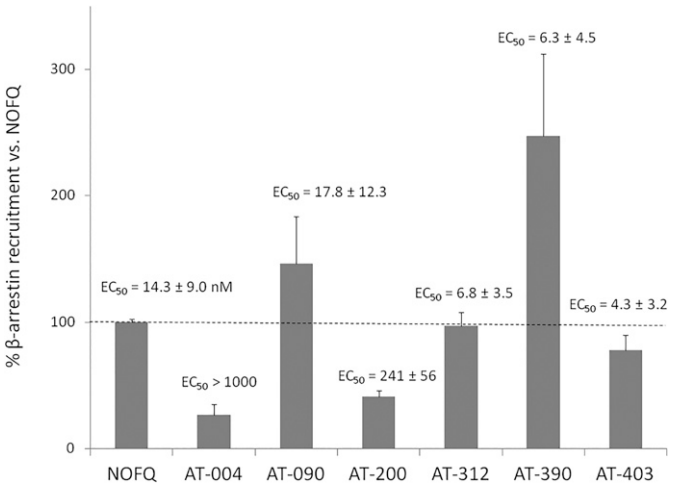

Fig. 4. Stimulation of β-arrestin recruitment at human NOP receptor induced by AT-004, AT-090, AT-200, AT-312, AT-390, and AT-403, normalized to N/OFQ (100%). On day 1, HTLA cells were plated at 10×10^6 cells in 150-mm cell culture dishes. On day 2, the cells were transfected with NOP receptor plasmids using the Fugene 6 HD transfection reagent. On day 3, transfected cells were harvested by trypsinization and then transferred into white flat-bottom 96-well tissue culture plates. On day 4, the cells were treated with corresponding AT compounds or N/OFQ control overnight at 37°C for at least 18 hours. On day 5, the luciferase reading in each well was detected by using a Bright Glo Luciferase Reporter Assay on a plate reader. Percentage of β-arrestin recruitment was normalized to that of N/OFQ (at 1 μM). Each experiment was repeated at least 3 times, with each drug concentration in quintuplicate wells to obtain the average value ± S.D. The potency (EC_{50} nM) of each NOP agonist for β-arrestin recruitment is labeled in the graph for each agonist.

internalization observed for these NOP agonists. Figure 5 shows a graphical representation of the relative levels of β-arrestin recruitment and internalization for each NOP agonist, including N/OFQ, at the NOP receptor. NOP full agonist AT-390 and NOP partial agonist AT-090 both show comparatively higher β-arrestin recruitment and internalization than N/OFQ, whereas the other NOP full agonists AT-403 and AT-312, as well as NOP partial agonists AT-004 and AT-200, showed lower β-arrestin recruitment and internalization. It is further notable that NOP full agonist AT-390, which shows higher β-arrestin recruitment and internalization than N/OFQ, shows no phosphorylation at any of the phosphosite residues we previously identified as being phosphorylated after N/OFQ binding (Mann et al., 2015). It is possible that residues other than the three phosphosites we probed with our available antibodies may be phosphorylated by NOP agonists such

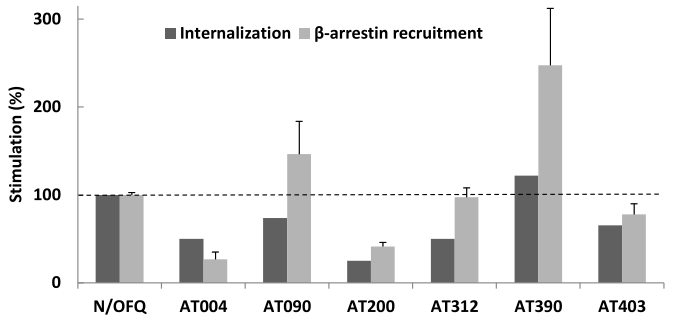

Fig. 5. Graphical side-by-side representation of the levels of NOP receptor internalization and β-arrestin recruitment by NOP agonists.

as AT-390 that lead to the robust β-arrestin recruitment and internalization observed with this nonpeptide NOP agonist.

Discussion

In this study, we characterized the intrinsic activity of chemically diverse NOP agonists in various G protein–mediated functional assays (GTPγS binding, cAMP inhibition, and GIRK activation) and characterized agonist-induced receptor trafficking by measuring ligand-induced NOP receptor phosphorylation of selected residues, arrestin recruitment, and receptor internalization. Targeting the NOP receptor has been proposed by us and others as an approach to reduce the side effects of MOR agonists (Bird and Lambert, 2015; Gunther et al., 2018; Kiguchi et al., 2020a; Kiguchi et al., 2020b; Toll et al., 2009). Using an array of ligands, we showed that NOP agonists with varying functional selectivity toward the MOR receptor, i.e., NOP-MOR bifunctional agonists, achieve antinociception comparable to that seen with MOR agonists but without the side effects of MOR such as opioid abuse liability, tolerance development, and respiratory depression (Ding et al., 2018; Sukhtankar et al., 2013; Toll et al., 2009; Vang et al., 2015). Selective NOP receptor full agonists such as AT-312 and AT-202 reduce rewarding effects of several abused substances such as alcohol, cocaine, and opioids (Toll et al., 2009; Zaveri et al., 2018a; Zaveri et al., 2018b). Other NOP full agonists such as AT-403 and AT-390 were found to attenuate the expression of levodopa-induced dyskinesia in animal models of Parkinson's disease (Arcuri et al., 2018). On the other hand, NOP receptor partial agonists such as AT-004 reduce Parkinsonian motor symptoms in hemilesioned rats (Kamakolanu et al., 2020), whereas partial agonists like AT-090 were shown to have antidepressant-like properties in animal models (Asth et al., 2016).

NOP full agonists AT-403 and the well-characterized NOP agonist Ro 64-6198 have been found to disrupt motor and neurologic function at higher doses (Arcuri et al., 2018; Higgins et al., 2001), an effect not observed with NOP partial agonists such as AT-004 or AT-090 (Asth et al., 2016; Kamakolanu et al., 2020). Since NOP receptor full agonists and partial agonists showed varying levels of separation between therapeutically relevant effects and apparent motor suppressive activity, we undertook the detailed in vitro assessment of functional efficacies of these NOP agonists in assays of NOP receptor function and trafficking. It was hoped that these tools could elucidate the signaling profiles of NOP receptor agonists and provide information on differential effects of receptor regulation that may help explain the pharmacological effects of these NOP agonists.

Among the selective NOP agonists we examined, AT-312, AT-390, and AT-403 behaved as full agonists in the GTPγS assay, whereas AT-004, AT-090, and AT-200 showed lower efficacy and were partial agonists in this assay (Table 2). All these compounds showed even lower efficacy in the MOR GTPγS binding assay, confirming their selectivity for NOP agonist efficacy over MOR efficacy (Table 2).

Interestingly, however, we consistently found that ligands that appeared as partial agonists in the GTPγS assay showed significantly higher efficacy and potency as nearly full agonists in the cAMP and GIRK assays (Table 2). Comparison of intrinsic activities from the GTPγS, cAMP, and GIRK assays revealed a systematically leftward

shift of all dose-response events in cAMP and GIRK assays (Fig. 2). The overestimation of agonist efficacy in the cAMP and GIRK assays was seen at both NOP and MOR receptors (Table 2). For example, although AT-004 showed only low efficacy for GTPγS binding at NOP, it behaved as a full agonist in the cAMP and GIRK assays (Table 2). Similarly, although AT-312 induced less than 30% stimulation in GTPγS binding at the MOR, it induced about 60% and > 70% stimulation in the MOR cAMP and GIRK assays, respectively. Similar results were also observed with other AT compounds (Table 2). It is possible that higher efficacy seen in the cAMP and GIRK assays is due to signal amplification downstream in the signaling pathway. Intrinsic activity (percentage of stimulation) measured in G protein assays using heterologous transfected cell lines is also known to be affected by receptor reserve and signal amplification (Adham et al., 1993; Baker et al., 2000; Harrison and Traynor, 2003; McDonald et al., 2003; McDonald and Lambert, 2010). These factors may play a role in the different levels of agonist efficacy measured in these assays (Nickolls et al., 2011; Selley et al., 1997).

According to the classic model of agonist-induced GPCR activation, the agonist-bound receptor, complexed with G proteins, is phosphorylated by GRKs and recruits β-arrestin, after which the receptor complex is targeted for internalization, leading to desensitization of the primary receptor signal. This study is the first to characterize several NOP agonists in these three main signaling nodes involved in NOP receptor trafficking after agonist binding, i.e., NOP receptor phosphorylation, β-arrestin recruitment, and internalization were studied for each ligand. Our data presented interesting differences in the ability of various NOP agonists to induce these events. NOP full agonist AT-403 showed robust phosphorylation of all three examined phosphosites (S346, S351, and S362/S363) of NOP receptor after 10 minutes of incubation, comparable to the natural NOP full agonist N/OFQ (Fig. 3A). NOP full agonist AT-312 also showed comparable phosphorylation at S346 and S351 but not at T362/S363 under similar exposure. NOP full agonist AT-390, on the other hand, showed no phosphorylation at any of these residues at any concentration under the same conditions. NOP partial agonists AT-004 and AT-200 showed minimal phosphorylation of NOP receptor residues S351 and T362/S363 at 10 μM concentration (Fig. 3A), whereas NOP partial agonist AT-090 showed a robust dose-dependent phosphorylation at all three sites after 10 minutes of incubation. The human NOP receptor contains several residues in its intracellular loops and C-terminal tail that can potentially be phosphorylated after receptor activation. Mann et al. (2015) reported that N/OFQ agonist-induced NOP phosphorylation occurs primarily within the residues in the C-terminal tail. They generated phosphosite-specific antibodies to the C-terminal residues S346, S351, and T362/S363 and showed that N/OFQ and nonpeptide agonists showed a hierarchical and temporal phosphorylation of S346 followed by S351 and T363/S363. In their study, the phosphorylation induced by N/OFQ and nonpeptide agonists appeared to correlate with the NOP internalization observed after treatment with these agonists. However, in the current study, the level of NOP internalization induced by the NOP agonists studied here did not appear to be consistent with the phosphorylation signatures induced by these agonists at the three phosphosites S346, S351, and T362/S363. Particularly, full agonist AT-390 showed no phosphorylation at any of these sites but still showed robust internalization compared to N/OFQ, which showed significant phosphorylation at all three residues. On the other hand, full agonist AT-403 showed similar phosphorylation to N/OFQ but lower internalization than N/OFQ (Fig. 3C). Although ligand-induced receptor phosphorylation was probed after 10 minutes of incubation, whereas internalization was measured after 60-minute exposure with NOP agonists, these results still suggest that residues other than S346, S351, and T362/S363 are likely involved in ligand-induced NOP phosphorylation, leading to subsequent internalization particularly for NOP full agonist AT-390. Given that opioid receptor internalization leads to receptor desensitization, NOP full agonist AT-390 may induce more NOP desensitization compared to full agonist AT-403, which may lead to differences in the pharmacological responses between these two NOP full agonists. Indeed, we found that AT-403 and AT-390 showed different windows of separation between their antidyskinetic effects and disruption of locomotor activity (Arcuri et al., 2018).

The efficacy and potency of β-arrestin recruitment by these NOP full agonists appeared to be consistent with the internalization induced by these agonists (Figs. 4 and 5). NOP full agonist AT-390 showed significantly higher arrestin recruitment with higher potency than the standard agonist N/OFQ. Interestingly, AT-390 also induces greater internalization than most other NOP full agonists we tested, including N/OFQ (Fig. 3C). In contrast, the chemically distinct NOP full agonist AT-403 shows lower arrestin recruitment than N/OFQ (Table 3; Supplemental Fig. 4F) and also lower internalization than N/OFQ.

NOP receptor partial agonists AT-004 and AT-200 did not show significant arrestin recruitment, but partial agonist AT-090 showed a robust recruitment of β-arrestin, with potency and efficacy greater than N/OFQ itself (Table 3; Supplemental Fig. 4). AT-090 also showed significant receptor phosphorylation and robust internalization compared with N/OFQ and other full agonists. Thus, among NOP partial agonists characterized in this study, the internalization induced by AT-090 may suggest a greater propensity for receptor desensitization than NOP partial agonists AT-004 and AT-200.

In summary, the characterization of structurally diverse NOP full agonists and partial agonists presented here highlights the differential functional effects of chemically diverse NOP agonists on ligand-induced receptor signaling and trafficking. Furthermore, the results demonstrate that measurement of intrinsic activities of agonist ligands can vary with the type of functional assay used to measure intrinsic activity. These differences are particularly pronounced in the case of partial agonist ligands, which can show varying levels of agonist efficacies depending on the assay and system used. Therefore, characterizing GPCR agonist ligands as full agonists or partial agonists must take into account several factors discussed above to determine intrinsic activity of agonist ligands. The differential effects on receptor trafficking, particularly of NOP full agonist AT-390 and NOP partial agonist AT-090, compared with other NOP agonists may be important to understand the pharmacological profiles and actions of these NOP agonists.

Acknowledgments

The kind gift of the HTLA cell line stably expressing a tetracycline-controlled transactivator-dependent luciferase reporter and a β-arrestin2–tobacco etch virus protease fusion gene, as well as corresponding plasmids for human NOP and MOR receptors, from Dr. Bryan Roth is gratefully acknowledged.

Authorship Contributions

Participated in research design: Lu, Mann, Schulz, Zaveri.

Conducted experiments: Lu, Polgar, Mann, Dasgupta.

Performed data analysis: Lu, Polgar, Mann, Dasgupta.

Wrote or contributed to the writing of the manuscript: Lu, Polgar, Schulz, Zaveri.

References

Adapa ID and Toll L (1997) Relationship between binding affinity and functional activity of nociceptin/orphanin FQ. *Neuropeptides* **31**:403–408.

Adham N, Ellerbrock B, Hartig P, Weinshank RL, and Branchek T (1993) Receptor reserve masks partial agonist activity of drugs in a cloned rat 5-hydroxytryptamine1B receptor expression system. *Mol Pharmacol* **43**:427–433.

Allen JA, Yost JM, Setola V, Chen X, Sassano MF, Chen M, Peterson S, Yadav PN, Huang XP, Feng B et al. (2011) Discovery of β-arrestin-biased dopamine D2 ligands for probing signal transduction pathways essential for antipsychotic efficacy. *Proc Natl Acad Sci USA* **108**:18488–18493.

Arcuri L, Novello S, Frassineti M, Mercatelli D, Pisanò CA, Morella I, Fasano S, Journigan BV, Meyer ME, Polgar WE et al. (2018) Anti-Parkinsonian and anti-dyskinetic profiles of two novel potent and selective nociceptin/orphanin FQ receptor agonists. *Br J Pharmacol* **175**:782–796.

Asth L, Ruzza C, Malfacini D, Medeiros I, Guerrini R, Zaveri NT, Gavioli EC, and Calo' G (2016) Beta-arrestin 2 rather than G protein efficacy determines the anxiolytic-versus antidepressant-like effects of nociceptin/orphanin FQ receptor ligands. *Neuropharmacology* **105**:434–442.

Baker SP, Scammells PJ, and Belardinelli L (2000) Differential A(1)-adenosine receptor reserve for inhibition of cyclic AMP accumulation and G-protein activation in DDT(1) MF-2 cells. *Br J Pharmacol* **130**:1156–1164.

Beedle AM, McRory JE, Poirot O, Doering CJ, Altier C, Barrere C, Hamid J, Nargeot J, Bourinet E, and Zamponi GW (2004) Agonist-independent modulation of N-type calcium channels by ORL1 receptors. *Nat Neurosci* **7**:118–125.

Bird MF and Lambert DG (2015) Simultaneous targeting of multiple opioid receptor types. *Curr Opin Support Palliat Care* **9**:98–102.

Bunzow JR, Saez C, Mortrud M, Bouvier C, Williams JT, Low M, and Grandy DK (1994) Molecular cloning and tissue distribution of a putative member of the rat opioid receptor gene family that is not a mu, delta or kappa opioid receptor type. *FEBS Lett* **347**:284–288.

Camarda V, Fischetti C, Anzellotti N, Molinari P, Ambrosio C, Kostenis E, Regoli D, Trapella C, Guerrini R, Severo S et al. (2009) Pharmacological profile of NOP receptors coupled with calcium signaling via the chimeric protein G alpha qi5. *Naunyn Schmiedebergs Arch Pharmacol* **379**:599–607.

Chang SD, Mascarella SW, Spangler SM, Gurevich VV, Navarro HA, Carroll FI, and Bruchas MR (2015) Quantitative signaling and structure-activity analyses demonstrate functional selectivity at the nociceptin/orphanin FQ opioid receptor. *Mol Pharmacol* **88**:502–511.

Cheng Y and Prusoff WH (1973) Relationship between the inhibition constant (K1) and the concentration of inhibitor which causes 50 per cent inhibition (I50) of an enzymatic reaction. *Biochem Pharmacol* **22**:3099–3108.

Connor M, Vaughan CW, Chieng B, and Christie MJ (1996a) Nociceptin receptor coupling to a potassium conductance in rat locus coeruleus neurones in vitro. *Br J Pharmacol* **119**:1614–1618.

Connor M, Yeo A, and Henderson G (1996b) The effect of nociceptin on Ca2+ channel current and intracellular Ca2+ in the SH-SY5Y human neuroblastoma cell line. *Br J Pharmacol* **118**:205–207.

Coward P, Chan SD, Wada HG, Humphries GM, and Conklin BR (1999) Chimeric G proteins allow a high-throughput signaling assay of Gi-coupled receptors. *Anal Biochem* **270**:242–248.

Ding H, Kiguchi N, Yasuda D, Daga PR, Polgar WE, Lu JJ, Czoty PW, Kishioka S, Zaveri NT, and Ko MC (2018) A bifunctional nociceptin and mu opioid receptor agonist is analgesic without opioid side effects in nonhuman primates. *Sci Transl Med* **10**:eaar3483.

Donica CL, Awwad HO, Thakker DR, and Standifer KM (2013) Cellular mechanisms of nociceptin/orphanin FQ (N/OFQ) peptide (NOP) receptor regulation and heterologous regulation by N/OFQ. *Mol Pharmacol* **83**:907–918.

Ferrari F, Cerlesi MC, Malfacini D, Asth L, Gavioli EC, Journigan BV, Kamakolanu UG, Meyer ME, Yasuda D, Polgar WE et al. (2016) In vitro functional characterization of novel nociceptin/orphanin FQ receptor agonists in recombinant and native preparations. *Eur J Pharmacol* **793**:1–13.

Ferrari F, Malfacini D, Journigan BV, Bird MF, Trapella C, Guerrini R, Lambert DG, Calo' G, and Zaveri NT (2017) In vitro pharmacological characterization of a novel unbiased NOP receptor-selective nonpeptide agonist AT-403. *Pharmacol Res Perspect* **5**: (in press).

Fukuda K, Kato S, Mori K, Nishi M, Takeshima H, Iwabe N, Miyata T, Houtani T, and Sugimoto T (1994) cDNA cloning and regional distribution of a novel member of the opioid receptor family. *FEBS Lett* **343**:42–46.

Gillis A, Sreenivasan V, and Christie MJ (2020) Intrinsic efficacy of opioid ligands and its importance for apparent bias, operational analysis and therapeutic window. *Mol Pharmacol* **98**:410–424.

Günther T, Culler M, and Schulz S (2016) Research resource: real-time analysis of somatostatin and dopamine receptor signaling in pituitary cells using a fluorescence-based membrane potential assay. *Mol Endocrinol* **30**:479–490.

Günther T, Dasgupta P, Mann A, Miess E, Kliewer A, Fritzwanker S, Steinborn R, and Schulz S (2018) Targeting multiple opioid receptors - improved analgesics with reduced side effects? *Br J Pharmacol* **175**:2857–2868.

Harrison C and Traynor JR (2003) The [35S]GTPgammaS binding assay: approaches and applications in pharmacology. *Life Sci* **74**:489–508.

Hawes BE, Graziano MP, and Lambert DG (2000) Cellular actions of nociceptin: transduction mechanisms. *Peptides* **21**:961–967.

Higgins GA, Grottick AJ, Ballard TM, Richards JG, Messer J, Takeshima H, Pauly-Evers M, Jenck F, Adam G, and Wichmann J (2001) Influence of the selective ORL1 receptor agonist, Ro64-6198, on rodent neurological function. *Neuropharmacology* **41**:97–107.

Hill SJ, Williams C, and May LT (2010) Insights into GPCR pharmacology from the measurement of changes in intracellular cyclic AMP; advantages and pitfalls of differing methodologies. *Br J Pharmacol* **161**:1266–1275.

Ikeda K, Kobayashi K, Kobayashi T, Ichikawa T, Kumanishi T, Kishida H, Yano R, and Manabe T (1997) Functional coupling of the nociceptin/orphanin FQ receptor with the G-protein-activated K+ (GIRK) channel. *Brain Res Mol Brain Res* **45**:117–126.

Kamakolanu UG, Meyer ME, Yasuda D, Polgar WE, Marti M, Mercatelli D, Pisanò CA, Brugnoli A, Morari M, and Zaveri NT (2020) Discovery and structure-activity relationships of nociceptin receptor partial agonists that afford symptom ablation in Parkinson's disease models. *J Med Chem* **63**:2688–2704.

Kelly E (2013) Efficacy and ligand bias at the μ-opioid receptor. *Br J Pharmacol* **169**:1430–1446.

Khroyan TV, Polgar WE, Orduna J, Montenegro J, Jiang F, Zaveri NT, and Toll L (2011) Differential effects of nociceptin/orphanin FQ (NOP) receptor agonists in acute versus chronic pain: studies with bifunctional NOP/μ receptor agonists in the sciatic nerve ligation chronic pain model in mice. *J Pharmacol Exp Ther* **339**:687–693.

Kiguchi N, Ding H, Kishioka S, and Ko MC (2020a) Nociceptin/orphanin FQ peptide receptor-related ligands as novel analgesics. *Curr Top Med Chem* **20**:2878–2888.

Kiguchi N, Ding H, and Ko MC (2020b) Therapeutic potentials of NOP and MOP receptor coactivation for the treatment of pain and opioid abuse. *J Neurosci Res* DOI: 10.1002/jnr.24624 [published online ahead of print]

Knapman A, Abogadie F, McIntrye P, and Connor M (2014) A real-time, fluorescence-based assay for measuring μ-opioid receptor modulation of adenylyl cyclase activity in Chinese hamster ovary cells. *J Biomol Screen* **19**:223–231.

Lachowicz JE, Shen Y, Monsma FJ Jr, and Sibley DR (1995) Molecular cloning of a novel G protein-coupled receptor related to the opiate receptor family. *J Neurochem* **64**:34–40.

Malfacini D, Ambrosio C, Gro' MC, Sbraccia M, Trapella C, Guerrini R, Bonora M, Pinton P, Costa T, and Calo' G (2015) Pharmacological profile of nociceptin/orphanin FQ receptors interacting with G-proteins and β-arrestins 2. *PLoS One* **10**:e0132865.

Mandyam CD, Thakker DR, Christensen JL, and Standifer KM (2002) Orphanin FQ/nociceptin-mediated desensitization of opioid receptor-like 1 receptor and mu opioid receptors involves protein kinase C: a molecular mechanism for heterologous cross-talk. *J Pharmacol Exp Ther* **302**:502–509.

Mandyam CD, Thakker DR, and Standifer KM (2003) Mu-opioid-induced desensitization of opioid receptor-like 1 and mu-opioid receptors: differential intracellular signaling determines receptor sensitivity. *J Pharmacol Exp Ther* **306**:965–972.

Mann A, Illing S, Miess E, and Schulz S (2015) Different mechanisms of homologous and heterologous μ-opioid receptor phosphorylation. *Br J Pharmacol* **172**:311–316.

Mann A, Moulédous L, Froment C, O'Neill PR, Dasgupta P, Günther T, Brunori G, Kieffer BL, Toll L, Bruchas MR et al. (2019) Agonist-selective NOP receptor phosphorylation correlates in vitro and in vivo and reveals differential post-activation signaling by chemically diverse agonists. *Sci Signal* **12**:eaau8072.

McDonald J, Barnes TA, Okawa H, Williams J, Calo' G, Rowbotham DJ, and Lambert DG (2003) Partial agonist behaviour depends upon the level of nociceptin/orphanin FQ receptor expression: studies using the ecdysone-inducible mammalian expression system. *Br J Pharmacol* **140**:61–70.

McDonald J and Lambert DG (2010) Binding of GTPgamma[35S] is regulated by GDP and receptor activation. Studies with the nociceptin/orphanin FQ receptor. *Br J Pharmacol* **159**:1286–1293.

Meunier JC, Mollereau C, Toll L, Suaudeau C, Moisand C, Alvinerie P, Butour JL, Guillemot JC, Ferrara P, Monsarrat B et al. (1995) Isolation and structure of the endogenous agonist of opioid receptor-like ORL1 receptor. *Nature* **377**:532–535.

Mollereau C, Parmentier M, Mailleux P, Butour JL, Moisand C, Chalon P, Caput D, Vassart G, and Meunier JC (1994) ORL1, a novel member of the opioid receptor family. Cloning, functional expression and localization. *FEBS Lett* **341**:33–38.

Nickolls SA, Waterfield A, Williams RE, and Kinloch RA (2011) Understanding the effect of different assay formats on agonist parameters: a study using the μ-opioid receptor. *J Biomol Screen* **16**:706–716.

Parsons MP and Hirasawa M (2011) GIRK channel-mediated inhibition of melanin-concentrating hormone neurons by nociceptin/orphanin FQ. *J Neurophysiol* **105**:1179–1184.

Reinscheid RK, Nothacker HP, Bourson A, Ardati A, Henningsen RA, Bunzow JR, Grandy DK, Langen H, Monsma FJ Jr, and Civelli O (1995) Orphanin FQ: a neuropeptide that activates an opioidlike G protein-coupled receptor. *Science* **270**:792–794.

Selley DE, Liu Q, and Childers SR (1998) Signal transduction correlates of mu opioid agonist intrinsic efficacy: receptor-stimulated [35S]GTP gamma S binding in mMOR-CHO cells and rat thalamus. *J Pharmacol Exp Ther* **285**:496–505.

Selley DE, Sim LJ, Xiao R, Liu Q, and Childers SR (1997) mu-Opioid receptor-stimulated guanosine-5′-O-(gamma-thio)-triphosphate binding in rat thalamus and

cultured cell lines: signal transduction mechanisms underlying agonist efficacy. *Mol Pharmacol* **51**:87–96.
Sim LJ, Xiao R, and Childers SR (1996) Identification of opioid receptor-like (ORL1) peptide-stimulated [35S]GTP gamma S binding in rat brain. *Neuroreport* **7**:729–733.
Sukhtankar DD, Zaveri NT, Husbands SM, and Ko MC (2013) Effects of spinally administered bifunctional nociceptin/orphanin FQ peptide receptor/μ-opioid receptor ligands in mouse models of neuropathic and inflammatory pain. *J Pharmacol Exp Ther* **346**:11–22.
Thakker DR and Standifer KM (2002) Induction of G protein-coupled receptor kinases 2 and 3 contributes to the cross-talk between mu and ORL1 receptors following prolonged agonist exposure. *Neuropharmacology* **43**:979–990.
Toll L, Bruchas MR, Calo' G, Cox BM, and Zaveri NT (2016) Nociceptin/orphanin FQ receptor structure, signaling, ligands, functions, and interactions with opioid systems. *Pharmacol Rev* **68**:419–457.
Toll L, Khroyan TV, Polgar WE, Jiang F, Olsen C, and Zaveri NT (2009) Comparison of the antinociceptive and antirewarding profiles of novel bifunctional nociceptin receptor/mu-opioid receptor ligands: implications for therapeutic applications. *J Pharmacol Exp Ther* **331**:954–964.
Traynor JR and Nahorski SR (1995) Modulation by mu-opioid agonists of guanosine-5′-O-(3-[35S]thio)triphosphate binding to membranes from human neuroblastoma SH-SY5Y cells. *Mol Pharmacol* **47**:848–854.
Vang D, Paul JA, Nguyen J, Tran H, Vincent L, Yasuda D, Zaveri NT, and Gupta K (2015) Small-molecule nociceptin receptor agonist ameliorates mast cell activation and pain in sickle mice. *Haematologica* **100**:1517–1525.
Vaughan CW and Christie MJ (1996) Increase by the ORL1 receptor (opioid receptor-like1) ligand, nociceptin, of inwardly rectifying K conductance in dorsal raphe nucleus neurones. *Br J Pharmacol* **117**:1609–1611.
Williams JT, Ingram SL, Henderson G, Chavkin C, von Zastrow M, Schulz S, Koch T, Evans CJ, and Christie MJ (2013) Regulation of μ-opioid receptors: desensitization, phosphorylation, internalization, and tolerance. *Pharmacol Rev* **65**:223–254.
Zaveri N, Polgar WE, Olsen CM, Kelson AB, Grundt P, Lewis JW, and Toll L (2001) Characterization of opiates, neuroleptics, and synthetic analogs at ORL1 and opioid receptors. *Eur J Pharmacol* **428**:29–36.
Zaveri NT, Jiang F, Olsen CM, Deschamps JR, Parrish D, Polgar W, and Toll L (2004) A novel series of piperidin-4-yl-1,3-dihydroindol-2-ones as agonist and antagonist ligands at the nociceptin receptor. *J Med Chem* **47**:2973–2976.
Zaveri NT, Marquez PV, Meyer ME, Hamid A, and Lutfy K (2018a) The nociceptin receptor (NOP) agonist AT-312 blocks acquisition of morphine- and cocaine-induced conditioned place preference in mice. *Front Psychiatry* **9**:638.
Zaveri NT, Marquez PV, Meyer ME, Polgar WE, Hamid A, and Lutfy K (2018b) A novel and selective nociceptin receptor (NOP) agonist (1-(1-((cis)-4-isopropylcyclohexyl) piperidin-4-yl)-1H-indol-2-yl)methanol (AT-312) decreases acquisition of ethanol-induced conditioned place preference in mice. *Alcohol Clin Exp Res* **42**:461–471.
Zhang NR, Planer W, Siuda ER, Zhao HC, Stickler L, Chang SD, Baird MA, Cao YQ, and Bruchas MR (2012) Serine 363 is required for nociceptin/orphanin FQ opioid receptor (NOPR) desensitization, internalization, and arrestin signaling. *J Biol Chem* **287**:42019–42030.

Address correspondence to: Nurulain T. Zaveri, Astraea Therapeutics, LLC., 320 Logue Avenue, Suite 142, Mountain View, CA 94043. E-mail: nurulain@astraeatherapeutics.com